The Surface Second-Harmonic Generation Yield

Sean M. Anderson[*] and Bernardo S. Mendoza[†]
Centro de Investigaciones en Óptica, A.C., León 37150, Mexico

Yujin Cho[‡]
Department of Physics, University of Texas at Austin, Austin, Texas 78712, USA

In this manuscript, we will walk through the considerations for developing the three layer (3-layer) model for the SSHG yield, which considers that the SH conversion takes place in a thin layer just below the surface that lies under the vacuum region and above the bulk of the material. We will then derive explicit expressions for each of the four polarization configurations for the incoming and outgoing fields. These expressions will be simplified by taking into account the symmetry relations for the (111), (110), and (001) surfaces. The reader can also consult the included Appendix that contains a wealth of supplementary derivations for all the work contained in this manuscript.

CONTENTS

I. THE THREE LAYER MODEL FOR THE SSHG YIELD

In this section, we will derive the formulas required for the calculation of the SSHG yield, defined by

$$\mathcal{R}(\omega) = \frac{I(2\omega)}{I^2(\omega)}, \tag{1.1}$$

with the intensity given by [1, 2]

$$I(\omega) = \begin{cases} \frac{c}{2\pi} n(\omega)|E(\omega)|^2 & \text{(CGS units)} \\ \\ 2\epsilon_0 c\, n(\omega)|E(\omega)|^2 & \text{(MKS units)} \end{cases}, \tag{1.2}$$

where $n(\omega) = \sqrt{\epsilon(\omega)}$ is the index of refraction ($\epsilon(\omega)$ is the dielectric function), ϵ_0 is the vacuum permittivity, and c the speed of light in vacuum.

---

* sma@cio.mx
† bms@cio.mx
‡ ycho@physics.utexas.edu

There are several ways to calculate $\mathcal{R}(\omega)$, one of which is the procedure followed by Cini [3]. This approach calculates the nonlinear susceptibility and at the same time the radiated fields. However, we present an alternative derivation based on the work of Mizrahi and Sipe [4], since the derivation of the 3-layer model is straightforward. In this scheme, the surface is represented by three regions or layers. The first layer is the vacuum region (denoted by v) with a dielectric function $\epsilon_v(\omega) = 1$ from where the fundamental electric field $\mathbf{E}_v(\omega)$ impinges on the material. The second layer is a thin layer (denoted by ℓ) of thickness d characterized by a dielectric function $\epsilon_\ell(\omega)$. It is in this layer where the SHG takes place. The third layer is the bulk region denoted by b and characterized by $\epsilon_b(\omega)$. Both the vacuum and bulk layers are semi-infinite (see Fig. 1).

To model the electromagnetic response of the 3-layer model, we follow Ref. [4] and assume a polarization sheet located at z_β, of the form

$$\mathbf{P}(\mathbf{r},t) = \boldsymbol{\mathcal{P}} e^{i\boldsymbol{\kappa}\cdot\mathbf{R}} e^{-i\omega t}\delta(z - z_\beta) + \text{c.c.}, \tag{1.3}$$

where $\mathbf{R} = (x, y)$, $\boldsymbol{\kappa}$ is the component of the wave vector $\boldsymbol{\nu}_\beta$ parallel to the surface, and z_β is the position of the sheet within medium β, and $\boldsymbol{\mathcal{P}}$ is the position-independent polarization. Ref. [5] demonstrates that the solution of the Maxwell equations for the radiated fields $E_{\beta,p\pm}$, and $E_{\beta,s}$ with $\mathbf{P}(\mathbf{r},t)$ as a source at points $z \neq 0$, can be written as

$$(E_{\beta,p\pm}, E_{\beta,s}) = \left(\frac{\gamma i\tilde{\omega}^2}{\tilde{w}_\beta}\,\hat{\mathbf{p}}_{\beta\pm}\cdot\boldsymbol{\mathcal{P}}, \frac{\gamma i\tilde{\omega}^2}{\tilde{w}_\beta}\,\hat{\mathbf{s}}\cdot\boldsymbol{\mathcal{P}}\right), \tag{1.4}$$

where $\gamma = 2\pi$ in CGS units or $\gamma = 1/2\epsilon_0$ in MKS units, and $\tilde{\omega} = \omega/c$. Also, $\hat{\mathbf{s}}$ and $\hat{\mathbf{p}}_{\beta\pm}$ are the unit vectors for the s and p polarizations of the radiated field, respectively. The $\pm$ refers to upward $(+)$ or downward $(-)$ direction of propagation within medium β, as shown in Fig. 1. Also, $\tilde{w}_\beta(\omega) = \tilde{\omega} w_\beta$, where

$$\hat{\mathbf{p}}_{\beta\pm}(\omega) = \frac{\kappa(\omega)\hat{\mathbf{z}} \mp \tilde{w}_\beta(\omega)\hat{\boldsymbol{\kappa}}}{\tilde{\omega} n_\beta(\omega)} = \frac{\sin\theta_0\hat{\mathbf{z}} \mp w_\beta(\omega)\hat{\boldsymbol{\kappa}}}{n_\beta(\omega)}, \tag{1.5}$$

with

$$w_\beta(\omega) = \left(\epsilon_\beta(\omega) - \sin^2\theta_0\right)^{1/2}, \tag{1.6}$$

θ_0 is the angle of incidence of $\mathbf{E}_v(\omega)$, $\kappa(\omega) = |\boldsymbol{\kappa}| = \tilde{\omega}\sin\theta_0$, $n_\beta(\omega) = \sqrt{\epsilon_\beta(\omega)}$ is the index of refraction of medium β, and z is the direction perpendicular to the surface that points towards the vacuum. If we consider the plane of

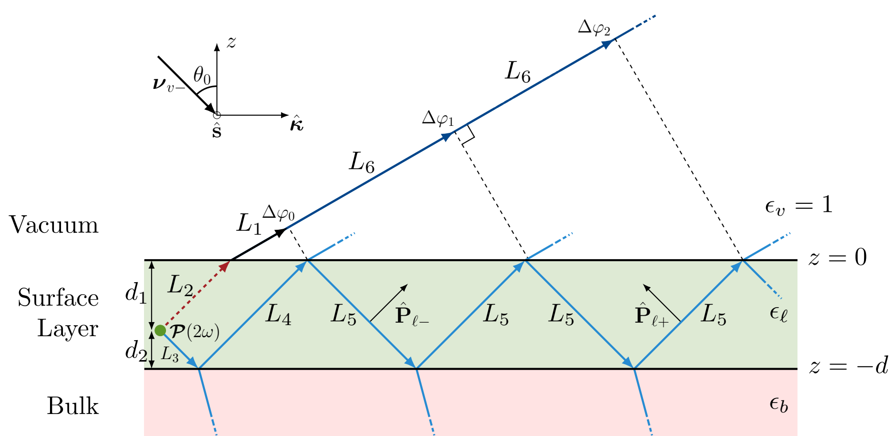

FIG. 1. Sketch of the three layer model for SHG. The vacuum region (v) is on top with $\epsilon_v = 1$; the layer ℓ of thickness $d = d_1 + d_2$, is characterized by $\epsilon_\ell(\omega)$, and it is where the SH polarization sheet $\boldsymbol{\mathcal{P}}_\ell(2\omega)$ is located at $z_\ell = d_1$. The bulk b is described by $\epsilon_b(\omega)$. The arrows point along the direction of propagation, and the p-polarization unit vector, $\hat{\mathbf{P}}_{\ell-(+)}$, along the downward (upward) direction is denoted with a thick arrow. The s-polarization unit vector $\hat{\mathbf{s}}$, points out of the page. The fundamental field $\mathbf{E}_v(\omega)$ is incident from the vacuum side along the $\hat{\boldsymbol{\kappa}}z$-plane, with θ_0 its angle of incidence and $\boldsymbol{\nu}_{v-}$ its wave vector. $\Delta\varphi_i$ denotes the phase difference between the multiple reflected beams and the first layer-vacuum transmitted beam, denoted by the dashed-red arrow (of length L_2) followed by the solid black arrow (of length L_1). The dotted lines in the vacuum region are perpendicular to the beam extended from the solid black arrow (denoted by solid blue arrows of length L_6).

incidence along the $\boldsymbol{\kappa}z$ plane, then

$$\hat{\boldsymbol{\kappa}} = \cos\phi\hat{\mathbf{x}} + \sin\phi\hat{\mathbf{y}}, \tag{1.7}$$

and

$$\hat{\mathbf{s}} = -\sin\phi\hat{\mathbf{x}} + \cos\phi\hat{\mathbf{y}}, \tag{1.8}$$

where ϕ is the azimuthal angle with respect to the x axis.

In the 3-layer model the nonlinear polarization responsible for the SHG is immersed in the thin layer ($\beta = \ell$), and is given by

$$\mathcal{P}^{\mathrm{a}}_{\ell}(2\omega) = \begin{cases} \chi^{\mathrm{abc}}_{\mathrm{surface}}(-2\omega;\omega,\omega)E^{\mathrm{b}}(\omega)E^{\mathrm{c}}(\omega) & \text{(CGS units)} \\ \epsilon_0\chi^{\mathrm{abc}}_{\mathrm{surface}}(-2\omega;\omega,\omega)E^{\mathrm{b}}(\omega)E^{\mathrm{c}}(\omega) & \text{(MKS units)} \end{cases}, \tag{1.9}$$

where $\boldsymbol{\chi}_{\mathrm{surface}}(-2\omega;\omega,\omega)$ is the dipolar surface nonlinear susceptibility tensor that we have derived in detail in Refs. [6, 7], and the Cartesian indices a, b, c are summed over if repeated. As we mentioned before, $\chi^{\mathrm{abc}}(-2\omega;\omega,\omega) = \chi^{\mathrm{acb}}(-2\omega;\omega,\omega)$ is the intrinsic permutation symmetry due to the fact that SHG is degenerate in $E^{\mathrm{b}}(\omega)$ and $E^{\mathrm{c}}(\omega)$. As in Ref. [4], we consider the polarization sheet (Eq. (1.3)) to be oscillating at some frequency ω in order to properly express Eqs. (1.4)-(1.8). However, in the following we find it convenient to use ω exclusively to denote the fundamental frequency and $\boldsymbol{\kappa}$ to denote the component of the incident wave vector parallel to the surface. The generated nonlinear polarization is oscillating at $\Omega = 2\omega$ and will be characterized by a wave vector parallel to the surface $\mathbf{K} = 2\boldsymbol{\kappa}$. We can carry over Eqs. (1.3)-(1.8) simply by replacing the lowercase symbols $(\omega, \tilde{\omega}, \boldsymbol{\kappa}, n_\beta, \tilde{w}_\beta, w_\beta, \hat{\mathbf{p}}_{\beta\pm}, \hat{\mathbf{s}})$ with uppercase symbols $(\Omega, \tilde{\Omega}, \mathbf{K}, N_\beta, \tilde{W}_\beta, W_\beta, \hat{\mathbf{P}}_{\beta\pm}, \hat{\mathbf{S}})$, all evaluated at 2ω. Of course, we always have that $\hat{\mathbf{S}} = \hat{\mathbf{s}}$.

From Fig. 1, we observe the propagation of the SH field as it is refracted at the layer-vacuum interface (ℓv), and reflected multiple times from the layer-bulk (ℓb) and layer-vacuum (ℓv) interfaces. Thus, we can define

$$\mathbf{T}^{\ell v} = \hat{\mathbf{s}}T^{\ell v}_s\hat{\mathbf{s}} + \hat{\mathbf{P}}_{v+}T^{\ell v}_p\hat{\mathbf{P}}_{\ell+}, \tag{1.10}$$

as the transmission tensor for the ℓv interface,

$$\mathbf{R}^{\ell b} = \hat{\mathbf{s}}R^{\ell b}_s\hat{\mathbf{s}} + \hat{\mathbf{P}}_{\ell+}R^{\ell b}_p\hat{\mathbf{P}}_{\ell-}, \tag{1.11}$$

as the reflection tensor for the ℓb interface, and

$$\mathbf{R}^{\ell v} = \hat{\mathbf{s}}R^{\ell v}_s\hat{\mathbf{s}} + \hat{\mathbf{P}}_{\ell-}R^{\ell v}_p\hat{\mathbf{P}}_{\ell+}, \tag{1.12}$$

as the reflection tensor for the ℓv interface. The Fresnel factors in uppercase letters, $T^{ij}_{s,p}$ and $R^{ij}_{s,p}$, are evaluated at 2ω from the following well known formulas [8]

$$\begin{aligned} t^{ij}_s(\omega) &= \frac{2w_i(\omega)}{w_i(\omega)+w_j(\omega)}, & t^{ij}_p(\omega) &= \frac{2w_i(\omega)\sqrt{\epsilon_i(\omega)\epsilon_j(\omega)}}{w_i(\omega)\epsilon_j(\omega)+w_j(\omega)\epsilon_i(\omega)}, \\ r^{ij}_s(\omega) &= \frac{w_i(\omega)-w_j(\omega)}{w_i(\omega)+w_j(\omega)}, & r^{ij}_p(\omega) &= \frac{w_i(\omega)\epsilon_j(\omega)-w_j\epsilon_i(\omega)}{w_i(\omega)\epsilon_j(\omega)+w_j(\omega)\epsilon_i(\omega)}. \end{aligned} \tag{1.13}$$

With these expressions we easily derive the following useful relations,

$$\begin{aligned} 1 + r^{\ell b}_s &= t^{\ell b}_s, \\ 1 + r^{\ell b}_p &= \frac{n_b}{n_\ell}t^{\ell b}_p, \\ 1 - r^{\ell b}_p &= \frac{n_\ell}{n_b}\frac{w_b}{w_\ell}t^{\ell b}_p, \\ t^{\ell v}_p &= \frac{w_\ell}{w_v}t^{v\ell}_p, \\ t^{\ell v}_s &= \frac{w_\ell}{w_v}t^{v\ell}_s. \end{aligned} \tag{1.14}$$

A. Multiple SHG Reflections

The SH field $\mathbf{E}(2\omega)$ radiated by the SH polarization $\boldsymbol{\mathcal{P}}_\ell(2\omega)$ will radiate directly into the vacuum and the bulk, where it will be reflected back at the layer-bulk interface into the thin layer. This beam will be transmitted and reflected multiple times, as shown in Fig. 1. As the two beams propagate, a phase difference will develop between them according to

$$\begin{aligned}\Delta\varphi_m &= \tilde{\Omega}\Big((L_3+L_4+2mL_5)N_\ell - \big(L_2N_\ell + (L_1+mL_6)N_v\big)\Big)\\ &= \delta_0 + m\delta, \quad m=0,1,2,\ldots,\end{aligned} \tag{1.15}$$

where

$$\delta_0 = 8\pi\left(\frac{d_2}{\lambda_0}\right)W_\ell, \tag{1.16}$$

and

$$\delta = 8\pi\left(\frac{d}{\lambda_0}\right)W_\ell, \tag{1.17}$$

where λ_0 is the wavelength of the fundamental field in the vacuum, W_ℓ is described in Eq. (1.6), d is the thickness of layer ℓ, and d_2 is the distance between $\boldsymbol{\mathcal{P}}_\ell(2\omega)$ and the ℓb interface (see Fig. 1). We see that δ_0 is the phase difference of the first and second transmitted beams, and $m\delta$ that of the first and third ($m=1$), first and fourth ($m=2$), and so on. Note that the thickness d of the layer ℓ enters through the phase δ, and the position d_2 of the nonlinear polarization $\mathbf{P}(\mathbf{r},t)$ (Eq. (1.3)) enters through δ_0. In particular, d_2 could be used as a variable to study the effects of multiple reflections on the SSHG yield $\mathcal{R}(2\omega)$.

To take into account the multiple reflections of the generated SH field in the layer ℓ, we proceed as follows. I include the algebra for the p-polarized SH field, and the s-polarized field could be worked out along the same steps. The p-polarized $\mathbf{E}_{\ell,p}(2\omega)$ field reflected multiple times is given by

$$\begin{aligned}\mathbf{E}_{\ell,p}(2\omega) &= E_{\ell,p+}(2\omega)\mathbf{T}^{\ell v}\cdot\hat{\mathbf{P}}_{\ell+} + E_{\ell,p-}(2\omega)\mathbf{T}^{\ell v}\cdot\mathbf{R}^{\ell b}\cdot\hat{\mathbf{P}}_{\ell-}e^{i\Delta\varphi_0}\\ &+ E_{\ell,p-}(2\omega)\mathbf{T}^{\ell v}\cdot\mathbf{R}^{\ell b}\cdot\mathbf{R}^{\ell v}\cdot\mathbf{R}^{\ell b}\cdot\hat{\mathbf{P}}_{\ell-}e^{i\Delta\varphi_1}\\ &+ E_{\ell,p-}(2\omega)\mathbf{T}^{\ell v}\cdot\mathbf{R}^{\ell b}\cdot\mathbf{R}^{\ell v}\cdot\mathbf{R}^{\ell b}\cdot\mathbf{R}^{\ell v}\cdot\mathbf{R}^{\ell b}\cdot\hat{\mathbf{P}}_{\ell-}e^{i\Delta\varphi_2}+\cdots\\ &= E_{\ell,p+}(2\omega)\mathbf{T}^{\ell v}\cdot\hat{\mathbf{P}}_{\ell+} + E_{\ell,p-}(2\omega)\mathbf{T}^{\ell v}\cdot\sum_{m=0}^{\infty}\Big(\mathbf{R}^{\ell b}\cdot\mathbf{R}^{\ell v}e^{i\delta}\Big)^m\cdot\mathbf{R}^{\ell b}\cdot\hat{\mathbf{P}}_{\ell-}e^{i\delta_0}.\end{aligned} \tag{1.18}$$

From Eqs. (1.10) - (1.12) it is easy to show that

$$\mathbf{T}^{\ell v}\cdot\Big(\mathbf{R}^{\ell b}\cdot\mathbf{R}^{\ell v}\Big)^n\cdot\mathbf{R}^{\ell b} = \hat{\mathbf{s}}T_s^{\ell v}\Big(R_s^{\ell b}R_s^{\ell v}\Big)^n R_s^{\ell b}\hat{\mathbf{s}} + \hat{\mathbf{P}}_{v+}T_p^{\ell v}\Big(R_p^{\ell b}R_p^{\ell v}\Big)^n R_p^{\ell b}\hat{\mathbf{P}}_{\ell-},$$

then,

$$\mathbf{E}_{\ell,p}(2\omega) = \hat{\mathbf{P}}_{\ell+}T_p^{\ell v}\Big(E_{\ell,p+}(2\omega) + \frac{R_p^{\ell b}e^{i\delta_0}}{1+R_p^{v\ell}R_p^{\ell b}e^{i\delta}}E_{\ell,p-}(2\omega)\Big), \tag{1.19}$$

where we used $R_{s,p}^{ij} = -R_{s,p}^{ji}$. Using Eq. (1.4) and (1.14), we can readily write

$$\mathbf{E}_{\ell,p}(2\omega) = \frac{\gamma i\tilde{\Omega}}{W_\ell}\mathbf{H}_\ell\cdot\boldsymbol{\mathcal{P}}_\ell(2\omega), \tag{1.20}$$

where

$$\mathbf{H}_\ell = \frac{W_\ell}{W_v}\left[\hat{\mathbf{s}}T_s^{v\ell}\left(1+R_s^M\right)\hat{\mathbf{s}} + \hat{\mathbf{P}}_{v+}T_p^{v\ell}\left(\hat{\mathbf{P}}_{\ell+} + R_p^M\hat{\mathbf{P}}_{\ell-}\right)\right], \tag{1.21}$$

and

$$R_{\mathrm{i}}^M \equiv \frac{R_{\mathrm{i}}^{\ell b}e^{i\delta_0}}{1+R_{\mathrm{i}}^{v\ell}R_{\mathrm{i}}^{\ell b}e^{i\delta}}, \quad \mathrm{i}=s,p, \tag{1.22}$$

is defined as the multiple (M) reflection coefficient. This coefficient depends on the thickness d of layer ℓ, and most importantly on the position d_2 of $\boldsymbol{\mathcal{P}}_\ell(2\omega)$ within this layer. The final results will depend on both d and d_2. However, using Eq. (1.16) we can also define an average $\bar{R}_{\rm i}^M$ as

$$\bar{R}_{\rm i}^M \equiv \frac{1}{d}\int_0^d \frac{R_{\rm i}^{\ell b} e^{i(8\pi W_\ell/\lambda_0)x}}{1+R_{\rm i}^{v\ell}R_{\rm i}^{\ell b}e^{i\delta}}\,dx = \frac{R_{\rm i}^{\ell b}e^{i\delta/2}}{1+R_{\rm i}^{v\ell}R_{\rm i}^{\ell b}e^{i\delta}}\,\mathrm{sinc}(\delta/2), \tag{1.23}$$

that only depends on d through the δ term from Eq. (1.17).

To connect with the work in Ref. [4], where $\boldsymbol{\mathcal{P}}(2\omega)$ is located on top of the vacuum-surface interface and only the vacuum radiated beam and the first (and only) reflected beam need be considered, we take $\ell = v$ and $d_2 = 0$, then $T^{\ell v} = 1$, $R^{v\ell} = 0$ and $\delta_0 = 0$, with which $R_{\rm i}^M = R_{\rm i}^{vb}$. Thus, Eq. (1.21) coincides with Eq. (3.8) of Ref. [4].

B. Multiple Reflections for the Linear Field

For a more complete formulation, we must also consider the multiple reflections of the fundamental field $\mathbf{E}_\ell(\omega)$ inside the thin ℓ layer. In Fig. 2 we present the situation where $\mathbf{E}_v(\omega)$ impinges from the vacuum side with an angle of incidence θ_0. As the first transmitted beam is multiply reflected from the ℓb and the ℓv interfaces, it accumulates a phase difference of $n\varphi$ (with $n = 1, 2, 3, \ldots$), and φ is given by

$$\begin{aligned}\varphi &= \frac{\omega}{c}(2L_1 n_\ell - L_2 n_v)\\ &= 4\pi\left(\frac{d}{\lambda_0}\right)w_\ell,\end{aligned} \tag{1.24}$$

where $n_v = 1$. We need Eqs. (1.11) and (1.12) for 1ω, and also need

$$\mathbf{t}^{v\ell} = \hat{\mathbf{s}}t_s^{v\ell}\hat{\mathbf{s}} + \hat{\mathbf{p}}_{\ell-}t_p^{v\ell}\hat{\mathbf{p}}_{v-}, \tag{1.25}$$

to write

$$\begin{aligned}\mathbf{E}_\ell(\omega) &= E_0\Big[\mathbf{t}^{v\ell} + \mathbf{r}^{\ell b}\cdot\mathbf{t}^{v\ell}e^{i\varphi} + \mathbf{r}^{\ell b}\cdot\mathbf{r}^{\ell v}\cdot\mathbf{r}^{\ell b}\cdot\mathbf{t}^{v\ell}e^{i2\varphi} + \mathbf{r}^{\ell b}\cdot\mathbf{r}^{\ell v}\cdot\mathbf{r}^{\ell b}\cdot\mathbf{r}^{\ell v}\cdot\mathbf{r}^{\ell b}\cdot\mathbf{t}^{v\ell}e^{i3\varphi} + \cdots\Big]\cdot\hat{\mathbf{e}}^{\rm i}\\ &= E_0\Big[1 + \Big(1 + \mathbf{r}^{\ell b}\cdot\mathbf{r}^{\ell v}e^{i\varphi} + (\mathbf{r}^{\ell b}\cdot\mathbf{r}^{\ell v})^2 e^{i2\varphi} + \cdots\Big)\cdot\mathbf{r}^{\ell b}e^{i\varphi}\Big]\cdot\mathbf{t}^{v\ell}\cdot\hat{\mathbf{e}}^{\rm i}\\ &= E_0\Big[\hat{\mathbf{s}}t_s^{v\ell}(1+r_s^M)\hat{\mathbf{s}} + t_p^{v\ell}\left(\hat{\mathbf{p}}_{\ell-} + \hat{\mathbf{p}}_{\ell+}r_p^M\right)\hat{\mathbf{p}}_{v-}\Big]\cdot\hat{\mathbf{e}}^{\rm i},\end{aligned} \tag{1.26}$$

where E_0 is the intensity of the fundamental field, and $\hat{\mathbf{e}}^{\rm i}$ is the unit vector of the incoming polarization, with $\mathrm{i} = s, p$, and then, $\hat{\mathbf{e}}^s = \hat{\mathbf{s}}$ and $\hat{\mathbf{e}}^p = \hat{\mathbf{p}}_{v-}$. Also,

$$r_{\rm i}^M \equiv \frac{r_{\rm i}^{\ell b}e^{i\varphi}}{1 + r_{\rm i}^{v\ell}r_{\rm i}^{\ell b}e^{i\varphi}}, \quad \mathrm{i} = s, p. \tag{1.27}$$

$r_{\rm i}^M$ is defined as the multiple (M) reflection coefficient for the fundamental field. We define $\mathbf{E}_\ell^{\rm i}(\omega) \equiv E_0\mathbf{e}_\ell^{\omega,\rm i}$ ($\mathrm{i} = s, p$), where

$$\mathbf{e}_\ell^{\omega,\rm i} = \Big[\hat{\mathbf{s}}t_s^{v\ell}(1+r_s^M)\hat{\mathbf{s}} + t_p^{v\ell}\left(\hat{\mathbf{p}}_{\ell-} + \hat{\mathbf{p}}_{\ell+}r_p^M\right)\hat{\mathbf{p}}_{v-}\Big]\cdot\hat{\mathbf{e}}^{\rm i}, \tag{1.28}$$

and using Eqs. (1.5), (1.7), and (1.8) we obtain that

$$\mathbf{e}_\ell^{\omega,i} = \left[t_s^{v\ell}r_s^{M+}\left(-\sin\phi\hat{\mathbf{x}} + \cos\phi\hat{\mathbf{y}}\right)\hat{\mathbf{s}} + \frac{t_p^{v\ell}}{n_\ell}\left(r_p^{M+}\sin\theta_0\hat{\mathbf{z}} + r_p^{M-}w_\ell\cos\phi\hat{\mathbf{x}} + r_p^{M-}w_\ell\sin\phi\hat{\mathbf{y}}\right)\hat{\mathbf{p}}_{v-}\right]\cdot\hat{\mathbf{e}}^{\rm i}, \tag{1.29}$$

where

$$r_{\rm i}^{M\pm} = 1 \pm r_{\rm i}^M, \quad \mathrm{i} = s, p. \tag{1.30}$$

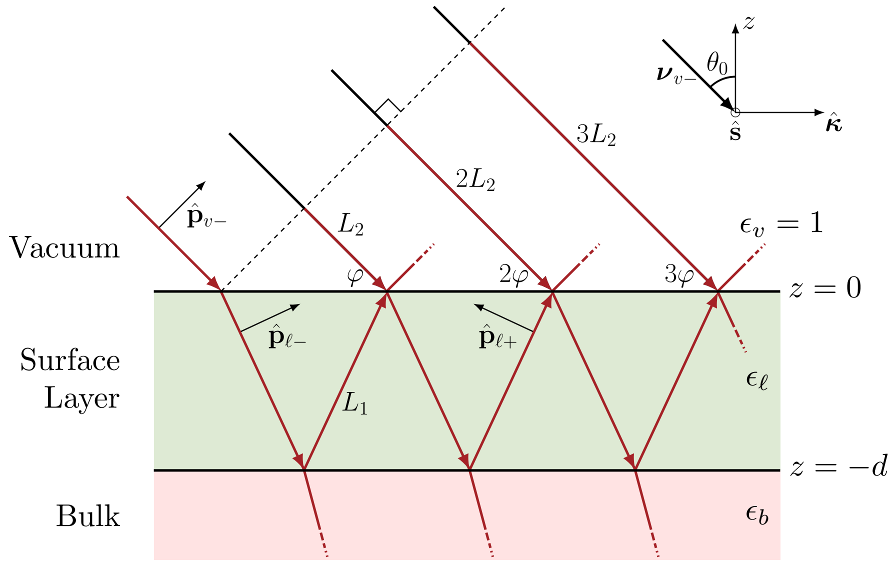

FIG. 2. Sketch for the multiple reflected fundamental field $\mathbf{E}_\ell(\omega)$, which impinges from the vacuum side along the $\hat{\boldsymbol{\kappa}}z$-plane. θ_0 and $\boldsymbol{\nu}_{v-}$ are the angle of incidence and wave vector, respectively. The arrows point along the direction of propagation. The p-polarization unit vectors $\hat{\mathbf{p}}_{\beta\pm}$, point along the downward $(-)$ or upward $(+)$ directions and are denoted with thick arrows, where $\beta = v$ or ℓ. The s-polarization unit vector $\hat{\mathbf{s}}$ points out of the page. $(1, 2, 3, \ldots)\varphi$ denotes the phase difference for the multiple reflected beams with respect to the incident field, where the dotted line is perpendicular to this beam.

C. Generalized Polarization Considerations for the Linear Field

Up until this juncture, we have not assumed any given polarization for the incoming fields, other than that they must be in some combination of p or s polarization. But let us consider the most general polarization case, elliptical polarization, by establishing that

$$\hat{\mathbf{e}}^{\mathrm{i}} = \sin\gamma\,\hat{\mathbf{s}} + e^{i\tau}\cos\gamma\,\hat{\mathbf{p}}_{v-}. \tag{1.31}$$

Plugging this into Eq. (1.29) yields

$$\mathbf{e}^{\omega}_{\ell} = \left[\sin\gamma\, t_s^{v\ell} r_s^{M+}\left(-\sin\phi\hat{\mathbf{x}} + \cos\phi\hat{\mathbf{y}}\right) + e^{i\tau}\cos\gamma\,\frac{t_p^{v\ell}}{n_\ell}\left(r_p^{M+}\sin\theta_0\hat{\mathbf{z}} + r_p^{M-}w_\ell\cos\phi\hat{\mathbf{x}} + r_p^{M-}w_\ell\sin\phi\hat{\mathbf{y}}\right)\right]. \tag{1.32}$$

The next section will make it clear that what we really need is $\mathbf{e}^{\omega}_{\ell}\mathbf{e}^{\omega}_{\ell}$. Multiplying these terms out leads to the following expression,

$$\begin{aligned}
\mathbf{e}^{\omega}_{\ell}\mathbf{e}^{\omega}_{\ell} = {} & \sin^2\gamma\,\left(t_s^{v\ell}r_s^{M+}\right)^2\left(\sin^2\phi\hat{\mathbf{x}}\hat{\mathbf{x}} + \cos^2\phi\hat{\mathbf{y}}\hat{\mathbf{y}} - 2\sin\phi\cos\phi\hat{\mathbf{x}}\hat{\mathbf{y}}\right)\\
& + e^{2i\tau}\cos^2\gamma\,\left(\frac{t_p^{v\ell}}{n_\ell}\right)^2\Bigg(\left(r_p^{M-}\right)^2 w_\ell^2\cos^2\phi\hat{\mathbf{x}}\hat{\mathbf{x}} + \left(r_p^{M-}\right)^2 w_\ell^2\sin^2\phi\hat{\mathbf{y}}\hat{\mathbf{y}} + \left(r_p^{M+}\right)^2\sin^2\theta_0\hat{\mathbf{z}}\hat{\mathbf{z}}\\
& \qquad + 2r_p^{M+}r_p^{M-}w_\ell\sin\theta_0\sin\phi\hat{\mathbf{y}}\hat{\mathbf{z}} + 2r_p^{M+}r_p^{M-}w_\ell\sin\theta_0\cos\phi\hat{\mathbf{x}}\hat{\mathbf{z}} + 2\left(r_p^{M-}\right)^2 w_\ell^2\sin\phi\cos\phi\hat{\mathbf{x}}\hat{\mathbf{y}}\Bigg)\\
& + 2e^{i\tau}\sin\gamma\cos\gamma\,\frac{t_p^{v\ell}t_s^{v\ell}r_s^{M+}}{n_\ell}\Big(-r_p^{M-}w_\ell\sin\phi\cos\phi\hat{\mathbf{x}}\hat{\mathbf{x}} + r_p^{M-}w_\ell\sin\phi\cos\phi\hat{\mathbf{y}}\hat{\mathbf{y}}\\
& \qquad + r_p^{M+}\sin\theta_0\cos\phi\hat{\mathbf{y}}\hat{\mathbf{z}} - r_p^{M+}\sin\theta_0\sin\phi\hat{\mathbf{x}}\hat{\mathbf{z}} + r_p^{M-}w_\ell\cos 2\phi\hat{\mathbf{x}}\hat{\mathbf{y}}\Big).
\end{aligned} \tag{1.33}$$

It is very convenient to switch over to a matrix representation. We can readily express the previous equation as a combination of vectors,

$$\mathbf{e}^{\omega}_{\ell}\mathbf{e}^{\omega}_{\ell} = \mathbf{CR}, \tag{1.34}$$

TABLE I. Values for γ and τ (see Eq. (1.31)) that yield common polarization cases.

Polarization	γ	τ
Linear – p	0	0
Linear – s	$\pi/2$	0
Linear – equal	$\pi/4$	0
Circular – left	$\pi/4$	$-\pi/2$
Circular – right	$\pi/4$	$+\pi/2$
Elliptical	Any	Any

where

$$\mathbf{C} = \left(\hat{\mathbf{x}}\hat{\mathbf{x}} \;\; \hat{\mathbf{y}}\hat{\mathbf{y}} \;\; \hat{\mathbf{z}}\hat{\mathbf{z}} \;\; \hat{\mathbf{y}}\hat{\mathbf{z}} \;\; \hat{\mathbf{x}}\hat{\mathbf{z}} \;\; \hat{\mathbf{x}}\hat{\mathbf{y}}\right), \tag{1.35}$$

and

$$\begin{aligned}\mathbf{R} = {} & \sin^2\gamma \left(t_s^{v\ell} r_s^{M+}\right)^2 \begin{pmatrix} \sin^2\phi \\ \cos^2\phi \\ 0 \\ 0 \\ 0 \\ -2\sin\phi\cos\phi \end{pmatrix} \\ & + e^{2i\tau}\cos^2\gamma \left(\frac{t_p^{v\ell}}{n_\ell}\right)^2 \begin{pmatrix} \left(r_p^{M-}\right)^2 w_\ell^2 \cos^2\phi \\ \left(r_p^{M-}\right)^2 w_\ell^2 \sin^2\phi \\ \left(r_p^{M+}\right)^2 \sin^2\theta_0 \\ 2r_p^{M+} r_p^{M-} w_\ell \sin\theta_0 \sin\phi \\ 2r_p^{M+} r_p^{M-} w_\ell \sin\theta_0 \cos\phi \\ 2\left(r_p^{M-}\right)^2 w_\ell^2 \sin\phi\cos\phi \end{pmatrix} \\ & + 2e^{i\tau}\sin\gamma\cos\gamma \, \frac{t_p^{v\ell} t_s^{v\ell} r_s^{M+}}{n_\ell} \begin{pmatrix} -r_p^{M-} w_\ell \sin\phi\cos\phi \\ r_p^{M-} w_\ell \sin\phi\cos\phi \\ 0 \\ r_p^{M+} \sin\theta_0\cos\phi \\ -r_p^{M+} \sin\theta_0 \sin\phi \\ r_p^{M-} w_\ell \cos 2\phi \end{pmatrix}.\end{aligned} \tag{1.36}$$

We list some common polarization cases in Table I C, and their respective values for γ and τ.

So, we have that Eq. (1.36) can encompass all possible polarization choices. We should be able to easily recover the expressions for p and s linear polarization. Plugging in the values for γ and τ featured in Table I C, we have that

$$\mathbf{e}_\ell^{\omega,p} = \frac{t_p^{v\ell}}{n_\ell}\left(r_p^{M+}\sin\theta_0\hat{\mathbf{z}} + r_p^{M-} w_\ell \hat{\boldsymbol{\kappa}}\right), \tag{1.37}$$

for p-input polarization with $\hat{\mathbf{e}}^{\mathrm{i}} = \hat{\mathbf{p}}_{v-}$, and

$$\mathbf{e}_\ell^{\omega,s} = t_s^{v\ell} r_s^{M+}\hat{\mathbf{s}}, \tag{1.38}$$

for s-input polarization with $\hat{\mathbf{e}}^{\mathrm{i}} = \hat{\mathbf{s}}$,

D. The SSHG Yield

The magnitude of the radiated field is given by $E(2\omega)=\hat{\mathbf{e}}^{\mathrm{F}}\cdot\mathbf{E}_\ell(2\omega)$, where $\hat{\mathbf{e}}^{\mathrm{F}}$ is the unit vector of the final, S or P SH polarization with $\mathrm{F}=S,P$, where $\hat{\mathbf{e}}^{S}=\hat{\mathbf{s}}$ and $\hat{\mathbf{e}}^{P}=\hat{\mathbf{P}}_{v+}$. We expand the rightmost term in parenthesis of Eq. (1.21) as

$$\begin{aligned}\hat{\mathbf{P}}_{\ell+}+R_p^M\hat{\mathbf{P}}_{\ell-}&=\frac{\sin\theta_0\hat{\mathbf{z}}-W_\ell\hat{\boldsymbol{\kappa}}}{N_\ell}+R_p^M\frac{\sin\theta_0\hat{\mathbf{z}}+W_\ell\hat{\boldsymbol{\kappa}}}{N_\ell}\\&=\frac{1}{N_\ell}\left(\sin\theta_0R_p^{M+}\hat{\mathbf{z}}-W_\ell R_p^{M-}\hat{\boldsymbol{\kappa}}\right),\end{aligned}\tag{1.39}$$

where

$$R_{\mathrm{i}}^{M\pm}\equiv 1\pm R_{\mathrm{i}}^M,\quad \mathrm{i}=s,p.\tag{1.40}$$

Using Eq. (1.14) we write Eq. (1.20) as

$$E_\ell(2\omega)=\frac{2\gamma i\omega}{cW_\ell}\hat{\mathbf{e}}^{\mathrm{F}}\cdot\mathbf{H}_\ell\cdot\boldsymbol{\mathcal{P}}_\ell(2\omega)=\frac{2\gamma i\omega}{cW_v}\mathbf{e}_\ell^{2\omega,\mathrm{F}}\cdot\boldsymbol{\mathcal{P}}_\ell(2\omega),\tag{1.41}$$

where

$$\mathbf{e}_\ell^{2\omega,\mathrm{F}}=\hat{\mathbf{e}}^{\mathrm{F}}\cdot\left[\hat{\mathbf{s}}T_s^{v\ell}R_s^{M+}\hat{\mathbf{s}}+\hat{\mathbf{P}}_{v+}\frac{T_p^{v\ell}}{N_\ell}\left(\sin\theta_0R_p^{M+}\hat{\mathbf{z}}-W_\ell R_p^{M-}\hat{\boldsymbol{\kappa}}\right)\right].\tag{1.42}$$

Replacing $\mathbf{E}_\ell(\omega)\to E_0\mathbf{e}_\ell^{\omega,\mathrm{i}}$, in Eq. (1.9), we obtain that

$$\boldsymbol{\mathcal{P}}_\ell(2\omega)=\begin{cases}E_0^2\,\boldsymbol{\chi}_{\mathrm{surface}}:\mathbf{e}_\ell^{\omega,\mathrm{i}}\mathbf{e}_\ell^{\omega,\mathrm{i}} & \text{(CGS units)}\\ \epsilon_0E_0^2\,\boldsymbol{\chi}_{\mathrm{surface}}:\mathbf{e}_\ell^{\omega,\mathrm{i}}\mathbf{e}_\ell^{\omega,\mathrm{i}} & \text{(MKS units)}\end{cases},\tag{1.43}$$

where $\mathbf{e}_\ell^{\omega,\mathrm{i}}$ is given by Eq. (1.28), and thus Eq. (1.41) reduces to ($W_v=\cos\theta_0$)

$$E_\ell(2\omega)=\frac{2\eta i\omega}{c\cos\theta_0}\mathbf{e}_\ell^{2\omega,\mathrm{F}}\cdot\boldsymbol{\chi}_{\mathrm{surface}}:\mathbf{e}_\ell^{\omega,\mathrm{i}}\mathbf{e}_\ell^{\omega,\mathrm{i}},\tag{1.44}$$

where $\eta=2\pi$ in CGS units and $\eta=1/2$ in MKS units. For ease of notation, we define

$$\Upsilon_{\mathrm{iF}}\equiv\mathbf{e}_\ell^{2\omega,\mathrm{F}}\cdot\boldsymbol{\chi}_{\mathrm{surface}}:\mathbf{e}_\ell^{\omega,\mathrm{i}}\mathbf{e}_\ell^{\omega,\mathrm{i}},\tag{1.45}$$

where i stands for the incoming polarization of the fundamental electric field given by $\hat{\mathbf{e}}^{\mathrm{i}}$ in Eq. (1.28), and F for the outgoing polarization of the SH electric field given by $\hat{\mathbf{e}}^{\mathrm{F}}$ in Eq. (1.42). I purposely omitted the full $\boldsymbol{\chi}(-2\omega;\omega,\omega)$ notation, and will do so from this point on.

From Eqs. (1.1) and (1.2) we obtain that in CGS units ($\eta=2\pi$),

$$\begin{aligned}|E(2\omega)|^2&=|E_0|^4\frac{16\pi^2\omega^2}{c^2W_v^2}|\Upsilon_{\mathrm{iF}}|^2\\ \frac{c}{2\pi}|\sqrt{N_v}E(2\omega)|^2&=\frac{32\pi^3\omega^2}{c^3\cos^2\theta_0}\left|\frac{\sqrt{N_v}}{n_\ell^2}\Upsilon_{\mathrm{iF}}\right|^2\left(\frac{c}{2\pi}|\sqrt{n_\ell}E_0|^2\right)^2\\ I(2\omega)&=\frac{32\pi^3\omega^2}{c^3\cos^2\theta_0}\left|\frac{\sqrt{N_v}}{n_\ell^2}\Upsilon_{\mathrm{iF}}\right|^2I^2(\omega)\\ \mathcal{R}_{\mathrm{iF}}(2\omega)&=\frac{32\pi^3\omega^2}{c^3\cos^2\theta_0}\left|\frac{1}{n_\ell}\Upsilon_{\mathrm{iF}}\right|^2,\end{aligned}\tag{1.46}$$

and in MKS units ($\eta = 1/2$),

$$
\begin{aligned}
|E(2\omega)|^2 &= |E_0|^4 \frac{\omega^2}{c^2 W_v^2} \\
2\epsilon_0 c|\sqrt{N_v} E(2\omega)|^2 &= \frac{2\epsilon_0\omega^2}{c\cos^2\theta_0} \left|\frac{\sqrt{N_v}}{n_\ell^2}\Upsilon_{\mathrm{iF}}\right|^2 \frac{1}{4\epsilon_0^2 c^2}\left(2\epsilon_0 c|\sqrt{n_\ell}E_0|^2\right)^2 \\
I(2\omega) &= \frac{\omega^2}{2\epsilon_0 c^3\cos^2\theta_0}\left|\frac{\sqrt{N_v}}{n_\ell^2}\Upsilon_{\mathrm{iF}}\right|^2 I^2(\omega) \\
\mathcal{R}_{\mathrm{iF}}(2\omega) &= \frac{\omega^2}{2\epsilon_0 c^3\cos^2\theta_0}\left|\frac{1}{n_\ell}\Upsilon_{\mathrm{iF}}\right|^2.
\end{aligned}
\tag{1.47}
$$

Finally, we condense these results and establish the SSHG yield as

$$
\mathcal{R}_{\mathrm{iF}}(2\omega)\begin{cases} \frac{32\pi^3\omega^2}{c^3\cos^2\theta_0}\left|\frac{1}{n_\ell}\Upsilon_{\mathrm{iF}}\right|^2 & \text{(CGS units)} \\ \\ \frac{\omega^2}{2\epsilon_0 c^3\cos^2\theta_0}\left|\frac{1}{n_\ell}\Upsilon_{\mathrm{iF}}\right|^2 & \text{(MKS units)}\end{cases}, \tag{1.48}
$$

where $N_v = 1$ and $W_v = \cos\theta_0$. $\boldsymbol{\chi}_{\mathrm{surface}}$ is given in m^2/V in the MKS unit system, since it is a surface second order nonlinear susceptibility, and $\mathcal{R}_{\mathrm{iF}}$ is given in m^2/W.

II. $\mathcal{R}_{\mathrm{iF}}$ FOR DIFFERENT POLARIZATION CASES

We now have everything we need to derive explicit expressions for $\mathcal{R}_{\mathrm{iF}}$, Eq. (1.48), for the most commonly used polarizations of incoming and outgoing fields (iF=pP, pS, sP, and sS). For this, we must expand Υ_{iF} from Eq. (1.45) for each case. By substituting Eqs. (1.7) and (1.8) into Eq. (1.42), we obtain

$$
\mathbf{e}_\ell^{2\omega,P} = \frac{T_p^{v\ell}}{N_\ell}\left(\sin\theta_0 R_p^{M+}\hat{\mathbf{z}} - W_\ell R_p^{M-}\cos\phi\hat{\mathbf{x}} - W_\ell R_p^{M-}\sin\phi\hat{\mathbf{y}}\right), \tag{2.1}
$$

for P ($\hat{\mathbf{e}}^{\mathrm{F}} = \hat{\mathbf{P}}_{v+}$) outgoing polarization, and

$$
\mathbf{e}_\ell^{2\omega,S} = T_s^{v\ell} R_s^{M+}\left(-\sin\phi\hat{\mathbf{x}} + \cos\phi\hat{\mathbf{y}}\right). \tag{2.2}
$$

for S ($\hat{\mathbf{e}}^{\mathrm{F}} = \hat{\mathbf{s}}$) outgoing polarization.

Following a similar procedure, we use Eqs. (1.7) and (1.8) with Eq. (1.37), and obtain

$$
\begin{aligned}
\mathbf{e}_\ell^{\omega,\mathrm{p}}\mathbf{e}_\ell^{\omega,\mathrm{p}} = \left(\frac{t_p^{v\ell}}{n_\ell}\right)^2 \Bigg(&\left(r_p^{M-}\right)^2 w_\ell^2\cos^2\phi\hat{\mathbf{x}}\hat{\mathbf{x}} + 2\left(r_p^{M-}\right)^2 w_\ell^2\sin\phi\cos\phi\hat{\mathbf{x}}\hat{\mathbf{y}} \\
&+2r_p^{M+}r_p^{M-}w_\ell\sin\theta_0\cos\phi\hat{\mathbf{x}}\hat{\mathbf{z}} + \left(r_p^{M-}\right)^2 w_\ell^2\sin^2\phi\hat{\mathbf{y}}\hat{\mathbf{y}} \\
&+2r_p^{M+}r_p^{M-}w_\ell\sin\theta_0\sin\phi\hat{\mathbf{y}}\hat{\mathbf{z}} + \left(r_p^{M+}\right)^2\sin^2\theta_0\hat{\mathbf{z}}\hat{\mathbf{z}}\Bigg),
\end{aligned}
\tag{2.3}
$$

for p incoming polarization ($\hat{\mathbf{e}}^{\mathrm{i}} = \hat{\mathbf{p}}_{v-}$), and with Eq. (1.38),

$$
\mathbf{e}_\ell^{\omega,\mathrm{s}}\mathbf{e}_\ell^{\omega,\mathrm{s}} = \left(t_s^{v\ell}r_s^{M+}\right)^2\left(\sin^2\phi\hat{\mathbf{x}}\hat{\mathbf{x}} + \cos^2\phi\hat{\mathbf{y}}\hat{\mathbf{y}} - 2\sin\phi\cos\phi\hat{\mathbf{x}}\hat{\mathbf{y}}\right). \tag{2.4}
$$

for s incoming polarization ($\hat{\mathbf{e}}^{\mathrm{i}} = \hat{\mathbf{s}}$).

We summarize the combination of equations needed to derive the expressions for all four polarization cases of $\mathcal{R}_{\mathrm{iF}}$ in Table II. In the following subsections we will derive the explicit expressions for Υ_{iF} for the most general case where the surface has no symmetry. We will then develop these expressions for particular cases of the most commonly investigated surfaces, the (111), (001) and (110) crystallographic faces. For ease of notation, we split Υ_{iF} as

$$
\Upsilon_{\mathrm{iF}} = \Gamma_{\mathrm{iF}}\, r_{\mathrm{iF}}, \tag{2.5}
$$

TABLE II. (Color online) Polarization unit vectors for $\hat{\mathbf{e}}^{\mathrm{F}}$ and $\hat{\mathbf{e}}^{\mathrm{i}}$, and equations describing $\mathbf{e}_\ell^{2\omega,\mathrm{F}}$ and $\mathbf{e}_\ell^{\omega,\mathrm{i}}\mathbf{e}_\ell^{\omega,\mathrm{i}}$ for each polarization case.

Case	$\hat{\mathbf{e}}^{\mathrm{F}}$	$\hat{\mathbf{e}}^{\mathrm{i}}$	$\mathbf{e}_\ell^{2\omega,\mathrm{F}}$	$\mathbf{e}_\ell^{\omega,\mathrm{i}}\mathbf{e}_\ell^{\omega,\mathrm{i}}$
$\mathcal{R}_{pP}$	$\hat{\mathbf{P}}_{v+}$	$\hat{\mathbf{p}}_{v-}$	Eq. (2.1)	Eq. (2.3)
$\mathcal{R}_{pS}$	$\hat{\mathbf{S}}$	$\hat{\mathbf{p}}_{v-}$	Eq. (2.2)	Eq. (2.3)
$\mathcal{R}_{sP}$	$\hat{\mathbf{P}}_{v+}$	$\hat{\mathbf{s}}$	Eq. (2.1)	Eq. (2.4)
$\mathcal{R}_{sS}$	$\hat{\mathbf{S}}$	$\hat{\mathbf{s}}$	Eq. (2.2)	Eq. (2.4)

and omit the "surface"subscript for the χ^{abc} components. A full, step-by-step derivation for all of these expressions can be found in Appendix **??**, with and without the effects of multiple reflections. The avid reader should refer to that chapter if interested in deriving any of the expressions listed below.

Many expressions can be greatly simplified by introducing a matrix representation for $\boldsymbol{\chi}$. Disregarding all symmetry relations, we have

$$\boldsymbol{\chi} = \begin{pmatrix} \chi^{xxx} & \chi^{xyy} & \chi^{xzz} & \vert & \chi^{xyz} & \chi^{xxz} & \chi^{xxy} \\ \chi^{yxx} & \chi^{yyy} & \chi^{yzz} & \vert & \chi^{yyz} & \chi^{yxz} & \chi^{yxy} \\ \chi^{zxx} & \chi^{zyy} & \chi^{zzz} & \vert & \chi^{zyz} & \chi^{zxz} & \chi^{zxy} \end{pmatrix}, \tag{2.6}$$

where all 18 independent components are accounted for, recalling that $\chi^{\mathrm{abc}} = \chi^{\mathrm{acb}}$ for SHG. Notice that the left hand block contains the components of χ^{abc} where $b = c$, and the right hand block those where $b \neq c$. As mentioned above, we are interested in the (111), (110) and (001) crystallographic faces, that belong to the C_{3v}, C_{2v}, and C_{4v} symmetry groups, respectively. For the (111) surface, we choose the x and y axes along the $[11\bar{2}]$ and $[1\bar{1}0]$ directions, respectively. For the (110) and (001), we consider the y axis perpendicular to the plane of symmetry.[9] These are represented in matrix form as

$$\boldsymbol{\chi}^{(111)} = \begin{pmatrix} \chi^{xxx} & -\chi^{xxx} & 0 & \vert & 0 & \chi^{xxz} & 0 \\ 0 & 0 & 0 & \vert & \chi^{xxz} & 0 & -\chi^{xxx} \\ \chi^{zxx} & \chi^{zxx} & \chi^{zzz} & \vert & 0 & 0 & 0 \end{pmatrix}, \tag{2.7}$$

$$\boldsymbol{\chi}^{(110)} = \begin{pmatrix} 0 & 0 & 0 & \vert & 0 & \chi^{xxz} & 0 \\ 0 & 0 & 0 & \vert & \chi^{yyz} & 0 & 0 \\ \chi^{zxx} & \chi^{zyy} & \chi^{zzz} & \vert & 0 & 0 & 0 \end{pmatrix}, \tag{2.8}$$

and

$$\boldsymbol{\chi}^{(001)} = \begin{pmatrix} 0 & 0 & 0 & \vert & 0 & \chi^{xxz} & 0 \\ 0 & 0 & 0 & \vert & \chi^{xxz} & 0 & 0 \\ \chi^{zxx} & \chi^{zxx} & \chi^{zzz} & \vert & 0 & 0 & 0 \end{pmatrix}. \tag{2.9}$$

In general, $\boldsymbol{\chi}^{(111)} \neq \boldsymbol{\chi}^{(110)} \neq \boldsymbol{\chi}^{(001)}$.

A. $\mathcal{R}_{pP}$ (p-in, P-out)

Per Table II, $\mathcal{R}_{pP}$ requires Eqs. (2.1) and (2.3). After some algebra, we obtain that

$$\Gamma_{pP} = \frac{T_p^{v\ell}}{N_\ell}\left(\frac{t_p^{v\ell}}{n_\ell}\right)^2, \tag{2.10}$$

and

$$r_{pP} = \begin{pmatrix} -R_p^{M-} W_\ell \cos\phi \\ -R_p^{M-} W_\ell \sin\phi \\ +R_p^{M+} \sin\theta_0 \end{pmatrix} \circ \boldsymbol{\chi} \cdot \begin{pmatrix} \left(r_p^{M-}\right)^2 w_\ell^2 \cos^2\phi \\ \left(r_p^{M-}\right)^2 w_\ell^2 \sin^2\phi \\ \left(r_p^{M+}\right)^2 \sin^2\theta_0 \\ 2r_p^{M+} r_p^{M-} w_\ell \sin\theta_0 \sin\phi \\ 2r_p^{M+} r_p^{M-} w_\ell \sin\theta_0 \cos\phi \\ 2\left(r_p^{M-}\right)^2 w_\ell^2 \sin\phi\cos\phi \end{pmatrix}, \tag{2.11}$$

where all 18 independent components of $\boldsymbol{\chi}$ can contribute to $\mathcal{R}_{pP}$. The "$\circ$" symbol is the Hadamard (piecewise) matrix product. For the (111) surface, we substitute Eq. (2.7) in Eq. (2.11) in lieu of $\boldsymbol{\chi}$ to obtain

$$\begin{aligned} r_{pP}^{(111)} = {} & R_p^{M+} \sin\theta_0 \Big[\left(r_p^{M+}\right)^2 \sin^2\theta_0 \chi^{zzz} + \left(r_p^{M-}\right)^2 w_\ell^2 \chi^{zxx} \Big] \\ & - R_p^{M-} w_\ell W_\ell \Big[2r_p^{M+} r_p^{M-} \sin\theta_0 \chi^{xxz} + \left(r_p^{M-}\right)^2 w_\ell \chi^{xxx} \cos 3\phi \Big], \end{aligned} \tag{2.12}$$

where the three-fold azimuthal symmetry of the SHG signal that is typical of the C_{3v} symmetry group is seen in the 3ϕ argument of the cosine function. For the (110) surface, we substitute Eq. (2.8) in Eq. (2.11) to obtain

$$\begin{aligned} r_{pP}^{(110)} = {} & R_p^{M+} \sin\theta_0 \left[\left(r_p^{M+}\right)^2 \sin^2\theta_0 \chi^{zzz} + \left(r_p^{M-}\right)^2 w_\ell^2 \left(\frac{\chi^{zyy} + \chi^{zxx}}{2} + \frac{\chi^{zyy} - \chi^{zxx}}{2} \cos 2\phi \right) \right] \\ & - 2R_p^{M-} r_p^{M+} r_p^{M-} w_\ell W_\ell \sin\theta_0 \left(\frac{\chi^{yyz} + \chi^{xxz}}{2} + \frac{\chi^{yyz} - \chi^{xxz}}{2} \cos 2\phi \right). \end{aligned} \tag{2.13}$$

The two-fold azimuthal symmetry of the SHG signal that is typical of the C_{2v} symmetry group, is seen in the 2ϕ argument of the cosine function. Lastly, for the (001) surface we simply make $\chi^{zxx} = \chi^{zyy}$ and $\chi^{xxz} = \chi^{yyz}$ (see Eqs. (2.8) and (2.9)), and the previous expression reduces to

$$r_{pP}^{(001)} = R_p^{M+} \sin\theta_0 \left[\left(r_p^{M+}\right)^2 \sin^2\theta_0 \chi^{zzz} + \left(r_p^{M-}\right)^2 w_\ell^2 \chi^{zxx} \right] - 2R_p^{M-} r_p^{M+} r_p^{M-} w_\ell W_\ell \sin\theta_0 \chi^{xxz}. \tag{2.14}$$

This time, the azimuthal 4ϕ symmetry for the C_{4v} group of the (001) surface is absent in this expression since this contribution is only related to the bulk nonlinear quadrupolar SH term,[9] which we neglect in this work.

B. $\mathcal{R}_{sP}$ (s-in, P-out)

Per Table II, $\mathcal{R}_{sP}$ requires Eqs. (2.1) and (2.4). After some algebra, we obtain that

$$\Gamma_{sP} = \frac{T_p^{v\ell}}{N_\ell} \left(t_s^{v\ell} r_s^{M+} \right)^2, \tag{2.15}$$

and

$$r_{sP} = \begin{pmatrix} -R_p^{M-} W_\ell \cos\phi \\ -R_p^{M-} W_\ell \sin\phi \\ +R_p^{M+} \sin\theta_0 \end{pmatrix} \circ \boldsymbol{\chi} \cdot \begin{pmatrix} \sin^2\phi \\ \cos^2\phi \\ 0 \\ 0 \\ 0 \\ -2\sin\phi\cos\phi \end{pmatrix}. \tag{2.16}$$

In this case, 9 out of the 18 components of $\boldsymbol{\chi}$ can contribute to $\mathcal{R}_{sP}$. This is because there is no $E_v^z(\omega)$ component, as the incoming polarization is s. As before, we substitute Eqs. (2.7), (2.8), and (2.9) in Eq. (2.16) to obtain

$$r_{sP}^{(111)} = R_p^{M+} \sin\theta_0 \chi^{zxx} + R_p^{M-} W_\ell \chi^{xxx} \cos 3\phi \tag{2.17}$$

for the (111) surface,

$$r_{sP}^{(110)} = R_p^{M+} \sin\theta_0 \left(\frac{\chi^{zxx} + \chi^{zyy}}{2} + \frac{\chi^{zyy} - \chi^{zxx}}{2} \cos 2\phi \right) \tag{2.18}$$

for the (110) surface, and

$$r_{sP}^{(001)} = R_p^{M+} \sin\theta_0 \chi^{zxx} \tag{2.19}$$

for the (001) surface.

C. $\mathcal{R}_{pS}$ (p-in, S-out)

Per Table II, $\mathcal{R}_{pS}$ requires Eqs. (2.2) and (2.3). After some algebra, we obtain that

$$\Gamma_{pS} = T_s^{v\ell} R_s^{M+} \left(\frac{t_p^{v\ell}}{n_\ell} \right)^2, \tag{2.20}$$

and

$$r_{pS} = \begin{pmatrix} -\sin\phi \\ \cos\phi \\ 0 \end{pmatrix} \circ \boldsymbol{\chi} \cdot \begin{pmatrix} \left(r_p^{M-}\right)^2 w_\ell^2 \cos^2\phi \\ \left(r_p^{M-}\right)^2 w_\ell^2 \sin^2\phi \\ \left(r_p^{M+}\right)^2 \sin^2\theta_0 \\ 2 r_p^{M+} r_p^{M-} w_\ell \sin\theta_0 \sin\phi \\ 2 r_p^{M+} r_p^{M-} w_\ell \sin\theta_0 \cos\phi \\ 2 \left(r_p^{M-}\right)^2 w_\ell^2 \sin\phi\cos\phi \end{pmatrix}, \tag{2.21}$$

In this case, 12 out of the 18 components of $\boldsymbol{\chi}$ can contribute to $\mathcal{R}_{pS}$. This is because there is no $\mathcal{P}_\ell^z(2\omega)$ component, as the outgoing polarization is S. As before, we substitute Eqs. (2.7), (2.8), and (2.9) in Eq. (2.21) to obtain

$$r_{pS}^{(111)} = -\left(r_p^{M-}\right)^2 w_\ell^2 \chi^{xxx} \sin 3\phi \tag{2.22}$$

for the (111) surface,

$$r_{pS}^{(110)} = r_p^{M+} r_p^{M-} w_\ell \sin\theta_0 (\chi^{yyz} - \chi^{xxz}) \sin 2\phi \tag{2.23}$$

for the (110) surface, and finally,

$$r_{pS}^{(001)} = 0 \tag{2.24}$$

for the (001) surface, where the zero value is only surface related, as we neglect the bulk nonlinear quadrupolar contribution.[9]

D. $\mathcal{R}_{sS}$ (s-in, S-out)

Per Table II, $\mathcal{R}_{sS}$ requires Eqs. (2.2) and (2.4). After some algebra, we obtain that

$$\Gamma_{sS} = T_s^{v\ell} R_s^{M+} \left(t_s^{v\ell} r_s^{M+}\right)^2, \tag{2.25}$$

and

$$r_{sS} = \begin{pmatrix} -\sin\phi \\ \cos\phi \\ 0 \end{pmatrix} \circ \boldsymbol{\chi} \cdot \begin{pmatrix} \sin^2\phi \\ \cos^2\phi \\ 0 \\ 0 \\ 0 \\ -2\sin\phi\cos\phi \end{pmatrix}. \tag{2.26}$$

In this case, only 6 out of the 18 components of $\boldsymbol{\chi}$ can contribute to $\mathcal{R}_{sS}$. This is because there is neither an $E_v^z(\omega)$ component as the incoming polarization is s, nor a $\mathcal{P}_\ell^z(2\omega)$ component as the outgoing polarization is S. As before, we substitute Eqs. (2.7), (2.8), and (2.9) in Eq. (2.26) to obtain

$$r_{sS}^{(111)} = \chi^{xxx}\sin 3\phi \tag{2.27}$$

for the (111) surface, and

$$r_{sS}^{(110)} = 0 \tag{2.28}$$

and

$$r_{sS}^{(001)} = 0 \tag{2.29}$$

for the (110) and (001) surfaces, respectively, both being zero as the bulk nonlinear quadrupolar contribution is not considered here.[9]

III. SOME SCENARIOS OF INTEREST

In this section we present five different scenarios for placing the nonlinear polarization $\boldsymbol{\mathcal{P}}(2\omega)$ and the fundamental electric field $\mathbf{E}(\omega)$, which are alternatives to the three-layer model presented above. In what follows, we confine ourselves only to the (111) surface and the p-in P-out combination polarizations. This is the case where the proposed scenarios differ the most as the SSHG yield depends on all the finite χ^{abc} components for this surface. However, the other pS, sP, and sS polarization cases, or the (110) or (001) surfaces could be worked out along the same lines described below. For all the scenarios we omit the multiple SH reflections by taking $R_p^{M\pm} \to 1 \pm R_p^{\ell b}$ (Eq. (1.40)) and the linear multiple reflections by taking $r_p^{M\pm} \to 1 \pm r_p^{\ell b}$ (Eq. (1.30)). Using the expressions in Eq. (1.14), we obtain the following useful relationships

$$\begin{aligned} r_p^{M+} &\to \frac{n_b}{n_\ell} t_p^{\ell b} \\ r_p^{M-} &\to \frac{n_\ell}{n_b}\frac{w_b}{w_\ell} t_p^{\ell b}, \end{aligned} \tag{3.1}$$

which will come in handy for expressing Γ_{pP} and $r_{pP}^{(111)}$ in the forms presented below. Recall that these expressions are valid for the 2ω terms by simply capitalizing the relevant quantities as explained in Sec. I. We summarize these scenarios in Table **??** for quick reference.

IV. CONCLUSIONS

In this manuscript, we derived the complete expressions for the SSHG radiation using the three layer model to describe the radiating system. Our derivation yields the full expressions for the radiation that include all required components of χ^{abc}, regardless of symmetry considerations. Thus, these expressions can be applied to any surface symmetry. We also reduce them according to the most commonly used surface symmetries, the (111), (110), and (100) cases.

[1] R.W. Boyd. *Nonlinear Optics.* Academic Press, New York, 2003.

[2] Richard L. Sutherland. *Handbook of Nonlinear Optics*. CRC Press, April 2003.
[3] Michele Cini. Simple model of electric-dipole second-harmonic generation from interfaces. *Phys. Rev. B*, 43(6):4792–4802, February 1991.
[4] V. Mizrahi and J. E. Sipe. Phenomenological treatment of surface second-harmonic generation. *J. Opt. Soc. Am. B*, 5(3):660–667, 1988.
[5] J. E. Sipe. New Green-function formalism for surface optics. *Journal of the Optical Society of America B*, 4(4):481–489, 1987.
[6] S. M. Anderson, N. Tancogne-Dejean, B. S. Mendoza, and V. Véniard. Theory of surface second-harmonic generation for semiconductors including effects of nonlocal operators. *Physical Review B*, 91(7):075302, February 2015.
[7] S. M. Anderson. *Theoretical Optical Second-Harmonic Calculations for Surfaces*. PhD thesis, Centro de Investigaciones en Óptica, A. C., Loma del Bosque 115, Colonia Lomas del Campestre León, Guanajuato 37150, Mexico, July 2016.
[8] J. D. Jackson. *Classical Electrodynamics, 3rd Edition*. Wiley-VCH, 3rd edition edition, July 1998.
[9] J. E. Sipe, D. J. Moss, and H. M. van Driel. Phenomenological theory of optical second- and third-harmonic generation from cubic centrosymmetric crystals. *Phys. Rev. B*, 35(3):1129–1141, January 1987.